

An inverse-geometry volumetric CT system with a large-area scanned source: A feasibility study

Taly Gilat Schmidt,^{a)} Rebecca Fahrig, and Norbert J. Pelc
Department of Radiology, Stanford University, Stanford, California 94305

Edward G. Solomon
NexRay Inc., Los Gatos, California 95032

(Received 26 November 2003; revised 23 April 2004; accepted for publication 7 July 2004; published 26 August 2004)

We propose an inverse-geometry volumetric CT system for acquiring a 15-cm volume in one rotation with negligible cone-beam artifacts. The system uses a large-area scanned source and a smaller detector array. This note describes two feasibility investigations. The first examines data sufficiency in the transverse planes. The second predicts the signal-to-noise ratio (SNR) compared to a conventional scanner. Results showed sufficient sampling of the full volume in less than 0.5 s and, when compared to a conventional scanner operating at 24 kW with a 0.5-s voxel illumination time (e.g., 0.5-s gantry rotation and pitch of one), predicted a relative SNR of 76%. © 2004 American Association of Physicists in Medicine. [DOI: 10.1118/1.1786171]

I. INTRODUCTION

Volumetric CT imaging was advanced significantly by the development of multiple-detector computed tomography (MDCT) systems. These systems provide faster scan times, thinner slices, and reduced motion artifacts compared to single-slice scanners.

The volume thickness covered in a single rotation by current MDCT scanners is still relatively small; for example these systems require many gantry rotations to image an entire organ such as the liver. In order to acquire a thicker volume per rotation, the detector extent in the axial direction (i.e., in the direction of the axis of rotation) must be increased, leading to a larger cone-beam angle. For a single rotation cone-beam acquisition (that is, a point x-ray source and an area detector rotated in a circle about the patient) an exact reconstruction is not possible because the acquired data set is insufficient.¹ Approximate reconstruction algorithms are available and generally used.² For small cone angles the resulting artifacts are negligible, but as the cone angle increases, so do the artifacts. A separate problem with this approach is that the detector array for such a system is necessarily very large. In order to support short scan times, the sampling rate for each element needs to be comparable to that of current clinical CT systems, raising concerns about cost.

This paper proposes an inverse-geometry volumetric CT system (IGCT) for acquiring a sufficient data set of a thick volume, on the order of several centimeters, in one subsecond gantry rotation. The proposed system uses a large-area scanned source array and a smaller array of fast detectors. In the transverse direction the sampling is fanlike, and in the axial direction the source and detector have the same extent, in principle providing a sufficient data set for accurate reconstruction.

We are proposing the IGCT system to achieve volumetric coverage in a single rotation while avoiding cone-beam artifacts. Another approach for achieving this is to use a 1D scanned source (scanned in the axial direction) with a large-

area detector array. While both approaches avoid data insufficiency problems, the IGCT system achieves this using a smaller detector array, which may provide significant scatter reduction and cost advantages.

The purpose of this technical note is to introduce the IGCT concept and to describe two feasibility investigations. The first examined whether sufficient sampling can be achieved in a scan time of 0.5 s or less. The second investigation determined whether enough photons are available to achieve a signal-to-noise ratio (SNR) comparable to that of a conventional MDCT scanner.

II. SYSTEM DESCRIPTION

The basic system geometry is illustrated in Fig. 1.

The proposed x-ray source has an electron beam that is electromagnetically steered across a transmission target, dwelling at a series of source locations. An array of collimator holes limits the x-ray beam produced at each location so that the beam illuminates only the detector. The detector is comprised of a smaller array of fast photon-counting detectors. For each source position, the entire detector array is read out producing a 2D divergent projection covering a fraction of the field of view (FOV). This is repeated for all source positions and for all gantry rotation angles. The scanning of the entire source is rapid compared to the rotation rate.

The source and detector arrays for the proposed system are conceptually similar to those used by NexRay, Inc., for their interventional cardiology C-arm system.³ In the IGCT system, the source and detector would be mounted on a gantry and rotated rapidly around the patient.

III. MATERIALS AND METHODS

A. Sampling

Since the source and detector of the IGCT system have the same axial extent, and assuming the spacing of source points and detectors in this direction is adequate, the sam-

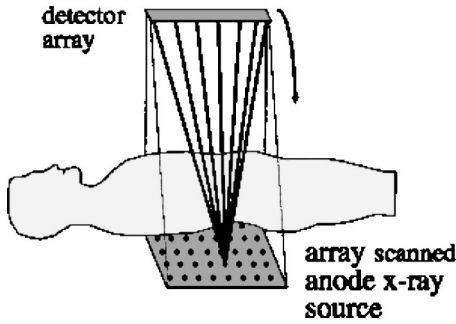


FIG. 1. Proposed IGCT geometry shown with the x-ray beam at one position in the source array.

pling in the slice direction is sufficient. The rays connecting each source with the row of detectors directly opposing it ensures this, and any additional oblique rays provide additional sampling, much as in 3D positron emission tomography (PET) imaging. The feasibility question being investigated is whether sufficient sampling in the transverse (or in-plane) direction can be acquired in a scan time of 0.5 s or less.

To answer this question it is helpful to consider the acquired data in Radon space. For a single-slice CT system, each ray can be described by two parameters, the rotation angle about the axis of rotation, ϕ , and the perpendicular distance to the center of rotation, ρ . The 1D projections can be represented in a 2D Radon space, with coordinates ρ and ϕ . A parallel-ray projection acquires a range of ρ values all at the same ϕ value, i.e., a horizontal line in Radon space. A single-slice fan-beam projection acquires a range of ρ values over a modest range of ϕ values (e.g., $\pm 20^\circ$). The samples form a curve in Radon space that for modest fan-beam angles is visually similar to a slanted line. A sufficient data set requires adequate sampling of all needed ρ values, based on the FOV and spatial resolution, and a range of ϕ values spanning at least π radians.

For the IGCT system, one “view” of in-plane samples can be defined as the rays connecting all source locations in a source row to all detectors in the opposed detector row. We define ψ to be the rotation angle of a ray in the absence of gantry rotation, as illustrated in Fig. 2. The ray connecting a source location s to a detector location d is defined by

$$\psi = \arctan\left(\frac{s-d}{SID+DID}\right), \tag{1}$$

$$\rho = d \cdot \cos(\psi) + DID \cdot \sin(\psi), \tag{2}$$

$$\phi = \psi + \phi_g, \tag{3}$$

where SID is the source-to-iso-center distance, DID is the detector-to-iso-center distance, and ϕ_g is the rotation angle of the gantry.

The rays connecting the entire source row with a single detector element form a fan, so the total sampling from a full view is a set of fans shifted in ρ and ϕ from each other, thereby forming a slanted swath in Radon space, as illustrated in Fig. 3. The fan formed by the upper detector ele-

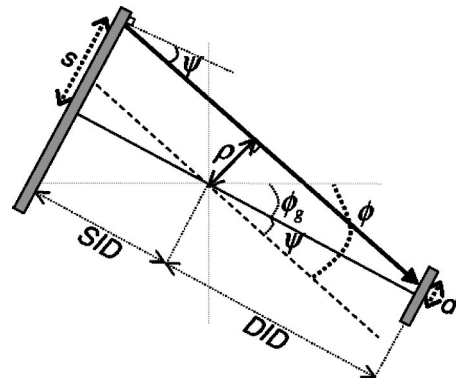


FIG. 2. The in-plane IGCT geometry with one source row and one detector row at a gantry rotation of ϕ_g . The ray connecting source location s and detector location d has an inherent rotation angle ψ , a total rotation angle ϕ , and is at a distance ρ from the isocenter.

ment (A in Fig. 3), contains the rays with largest positive ρ and most negative ϕ (with clockwise being the positive rotation direction). Moving towards the lower detector element, the fans shift in the negative ρ and positive ϕ directions.

As the gantry rotates, the next scan of the same source row generates a new swath in Radon space. In order to have a sufficient data set, enough views must be acquired so that there are no gaps between swaths. For a desired scan time, the number of views is limited by the time needed to scan the source which includes the dwell time at each source location and the beam steering time. The detector read out is overlapped with the beam steering and therefore does not impact the total scan time. We examined this sampling using the timing parameters of the NexRay source³ and also considered the impact of sequential versus nonsequential sampling of the source rows.

B. Photon flux and signal-to-noise ratio

The SNR in a CT image depends on the number of photons that passed through a resolution element and were de-

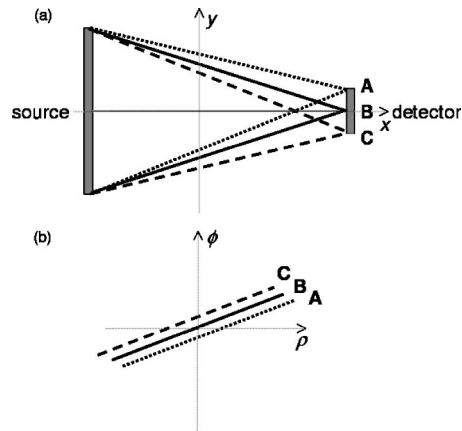


FIG. 3. The fans formed by (a) connecting a detector element in the detector row to the entire source row and (b) the corresponding sampling in Radon space. The fans from all detector elements sample a slanted swath of Radon space.

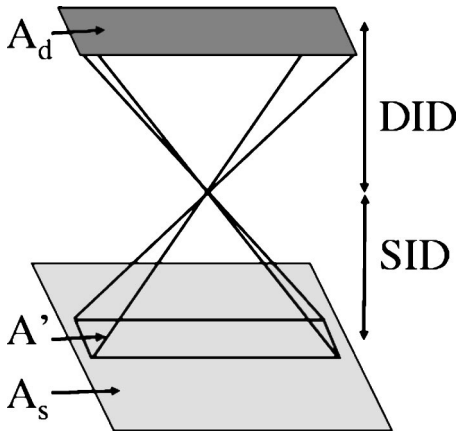


FIG. 4. The effective area of the source, A' , for a voxel in the object, where A_s and A_d are the areas of the source and detector, respectively.

tected, and the spatial resolution of the system. For this preliminary investigation, the question of SNR was studied by determining whether the proposed system can provide enough photon flux as compared to a conventional MDCT scanner.

We first analyzed the relative usable x-ray flux of the IGCT system compared to a conventional scanner. We define this as the number of photons per mA that illuminate a voxel. In this analysis we assume that the voxel is at isocenter, and we expect the results to be similar throughout the FOV. In a conventional scanner, each voxel in the FOV is illuminated by the source continuously as long as the voxel is within the axial coverage of the x-ray beam, while in the IGCT system, the voxel is only illuminated by a fraction of the source locations, for example when the source is in the area illustrated as A' in Fig. 4. This effective area, A' , which is the detector area, A_d , magnified onto the source, depends on the SID and the DID,

$$A' = A_d \cdot \frac{SID^2}{DID^2}. \tag{4}$$

Therefore, in the IGCT geometry, a voxel is illuminated for a fraction of the scan time equal to the ratio of A' to A_s , and the relative usable x-ray flux is proportional to this ratio. Also in the IGCT system, the x-ray beam is turned off while the beam is moved from one location to another, which can be accounted for by f_{duty} , the fraction of the time the scanned source produces x rays (i.e., one minus the fraction of the time spent moving the source from one location to another). Conventional x-ray tubes use “reflection” targets while the proposed system uses a transmission target, and there are differences in the Bremsstrahlung emissions for these two approaches.³ The relative efficiency of the Bremsstrahlung emission of the transmission target compared to a reflection target can be expressed using the factor f_x . In both systems, the number of photons at the object is inversely proportional to SID^2 . Combining these parameters, the relative usable x-ray flux of the IGCT system compared to a conventional MDCT scanner, F_{rel} , is

TABLE I. Specifications for preliminary investigated IGCT geometry.

Source dimensions (transverse×axial)	50×15 cm
Number of source locations	200×60
Detector dimensions (transverse×axial)	5×15 cm
Number of detector elements	48×144
Dwell time per source location	1 μ s
Move time between successive source locations	0.28 μ s
Source power	96 kW
Gantry rotation time	0.5 s
SID	41 cm
DID	54 cm
FOV (transverse×axial)	30 cm×15 cm

$$F_{rel} = \frac{A'}{A_s} \left(\frac{SID_{conv}}{SID} \right)^2 \cdot f_x \cdot f_{duty}. \tag{5}$$

In the IGCT system, the FOV in the transverse direction, FOV_t , depends on the transverse source extent and the magnification, while in the axial direction, since the source and detector have the same extent, the field of view, FOV_a , is equivalent to the axial source extent. The source area, A_s , can be expressed in terms of the total FOV,

$$A_s = \frac{FOV_t \cdot FOV_a \cdot (SID + DID)}{DID}. \tag{6}$$

Equations (4)–(6) can be used to calculate the relative usable x-ray flux of the IGCT system compared to a MDCT system. We now assume that the two geometries have the same magnification and source-to-detector distance. Because of the inverted geometry, this implies that the SID of the IGCT system is equivalent to the DID of the conventional system. Using this relationship along with Eqs. (4) and (6), Eq. (5) can be written as

$$F_{rel} = \frac{A_d \cdot DID}{FOV_t \cdot FOV_a \cdot (SID + DID)} \cdot f_x \cdot f_{duty}. \tag{7}$$

The relative SNR is proportional to the square root of the total number of photons, which depends on the relative usable x-ray flux, the relative detective quantum efficiency, DQE_{rel} , the relative power, P_{rel} , and the relative exposure times, T_{rel} , of the two systems

$$SNR_{rel} = \sqrt{F_{rel} \cdot DQE_{rel} \cdot P_{rel} \cdot T_{rel}}. \tag{8}$$

Note that for determining T_{rel} , the exposure time for a MDCT system scanning in helical mode is the time during which a resolution element is irradiated, which is a fraction of the total scan time.

Together, Eqs. (7) and (8) provide an analytical method for examining the SNR feasibility of the IGCT system.

C. Investigated geometry

The specifications of the analyzed IGCT system are given in Table I. The values are based on the current NexRay components, with some reasonable modifications to support a CT application. The source and detector dimensions have been

TABLE II. Specifications for comparison MDCT geometry.

Source power	24 kW
Voxel illumination time	0.5 s
Gantry rotation time	0.5 s
Helical pitch	1
SID	54 cm
DID	41 cm

modified in the proposed system to provide the desired FOV. The source power has also been increased by assuming a 0.6-mm source focal spot as opposed to the current 0.3-mm focal spot. The relevant MDCT specifications which factor into Eqs. (7) and (8) are listed in Table II. The MDCT detector size, scanning mode, and gantry rotation time determine the voxel illumination time but otherwise do not affect the SNR calculation.

IV. RESULTS

A. Sampling

Using the parameters in Table I, 0.256 ms is needed to scan each source row, and 15.4 ms is needed to scan the entire source array. Therefore the complete source array can be scanned a total of 32 times during a 0.5 s scan.

Figure 5(a) shows the in-plane sampling of Radon space from one row in one view, calculated using Eqs. (1)–(3) and Table I. This calculation assumes that the gantry is being continuously rotated at a speed of 4π radians/second.

During an acquisition, the remaining source rows in the array are scanned before this particular row is rescanned 15.4

ms later. During this time, the gantry rotates 0.19 radians. Figure 5(b) shows the Radon space coverage from the initial scan of the source row, and from the same source row 15.4 ms later. This sampling scheme is insufficient, as a gap exists between the swaths. This problem is not due to an insufficient number of measurements but rather a poor distribution. In fact, each swath in Radon space is oversampled.

The sequential scanning of source rows as simulated above is inefficient because the information acquired by two adjacent source rows is very similar. That is, a resolution element in the scanned volume is sampled through very similar ray paths by the two adjacent source rows. Therefore, scanning these two rows consecutively in time yields nearly redundant data. A better method for scanning the source is to interleave the source row order, for example scanning first the odd source rows, followed by the even source rows. Figure 5(c) shows the Radon space coverage of the first source and detector rows, and the sampling of the adjacent source and detector rows after all the odd rows have been scanned. The gap in Radon space has been removed, and in fact the swaths overlap suggesting that the scan time can be shortened. Therefore, by using interlaced source scanning, sufficient data can be acquired for the 15-cm volume in less than 0.5 s.

B. Photon flux and signal-to-noise ratio

Using a transmission x-ray target improves photon generation by a factor of 1.7 compared to a reflection target.³ Assuming the specifications in Tables I and II, Eq. (7) yields a relative usable x-ray flux of 0.12, meaning that the proposed system has approximately one tenth of the flux of a conventional system, within the volume that each is illuminating during a single rotation. Note that when scanning a large volume, the MDCT system does not illuminate the entire volume during the full scan time.

To understand the implications of this photon flux on image quality, the relative SNR can be calculated using Eq. (8). We assume that the comparison MDCT system operates at 24 kW with each voxel in the volume illuminated for 0.5 s, for example a MDCT system with a 0.5 s gantry rotation and a helical pitch of one. The assumed DQE of the photon-counting detector used in the IGCT system was 1.2 times that of a conventional detector.⁴ Using the relative usable x-ray flux, the relative DQE, and the scan time, power level, and other specifications listed in Tables I and II, the SNR of the IGCT system is predicted to be 76% of the SNR of a conventional MDCT system.

This analysis shows that the SNR of the proposed system is of the same order as that of a MDCT system. Note that the IGCT system achieves this performance in a single rotation while the MDCT system needs multiple rotations to cover the same volume. As can be seen from Eqs. (7) and (8), this comparison depends strongly on the design parameters. For example, increasing the detector size in the transverse direction can quickly improve the relative flux and SNR by increasing the solid angle subtended by each source location. The SNR can also be increased by lengthening the scan time.

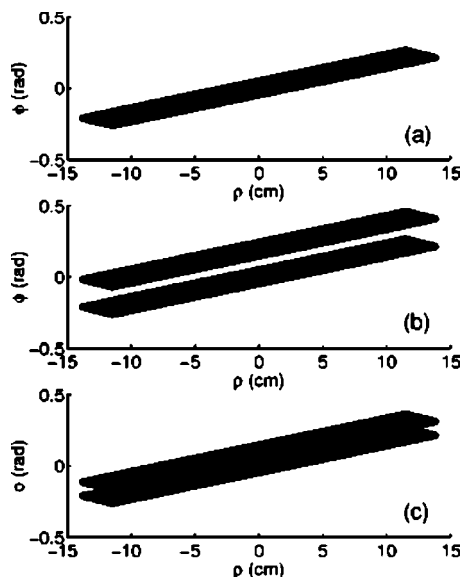


FIG. 5. For all plots, the gantry is rotating continuously at 4π radians per second. (a) The swath in Radon space representing the in-plane samples of the IGCT system, that is, all rays connecting each position in one source row to all the elements in the opposing detector row. (b) The first swath and the additional swath sampled by the same source and detector rows after the entire source array has been scanned. (c) The first swath and the swath sampled by the adjacent source and detector rows after half of the source rows have been scanned.

V. DISCUSSION AND CONCLUSIONS

This paper proposes an inverse-geometry volumetric CT system that uses a large-area scanned source. The proposed system can acquire a 15-cm volume thickness in one circular scan. Although more work is needed to understand the performance of the system, the preliminary investigations described in this note demonstrate feasibility in two areas. The sampling investigation establishes that sufficient sampling is possible at scan times of less than 0.5 s. The SNR calculation predicts noise performance comparable to a conventional MDCT scanner. Of note, this SNR is achieved for a volumetric scan in a single rotation, while the MDCT system needs multiple rotations for the same volumetric coverage and SNR.

One important aspect that was not discussed above is an appropriate reconstruction method to use for the acquired data set. This is beyond the scope of the present paper. However, it should be noted that the data set from the IGCT system is very similar to that from a multiring PET system, and therefore a PET reconstruction algorithm could be used for the IGCT system.^{5,6} We are exploring the use of a reconstruction method using rebinning to 2D parallel-ray projections.

The results of this preliminary investigation are very encouraging, but significant challenges remain. In addition to the algorithm work, the sampling and SNR predictions of the

present analysis need to be confirmed with simulations and experimental measurements on a bench top system. Because of the relationship between the source size and the FOV, achieving a large in-plane FOV with an IGCT system while maintaining a fast scan time will be challenging. Finally, construction of a prototype will require significant engineering work, including design solutions for mounting the components on the gantry and for transferring the large data set from the rotating gantry. Nonetheless, the IGCT concept is promising, and offers the possibility of high-speed volumetric imaging with freedom from cone-beam artifacts.

^{a)}Also at Department of Electrical Engineering, Stanford University, Stanford, California 94305.

¹B. D. Smith, "Cone-beam tomography: Recent advances and a tutorial review," *Opt. Eng.* **29**, 524–534 (1990).

²L. A. Feldkamp, L. C. Davis, and J. W. Kress, "Practical cone-beam algorithm," *J. Opt. Soc. Am. A* **1**, 612–619 (1984).

³E. G. Solomon, B. P. Wilfley, M. S. Van Lysel, A. W. Joseph, and J. A. Heanue, "Scanning-beam digital x-ray (SBDX) system for cardiac angiography," in *Medical Imaging 1999: Physics of Medical Imaging* (SPIE, New York, 1999), Vol. 3659, pp. 246–257.

⁴M. J. Tapiovaara and R. F. Wagner, "SNR and DQE analysis of broad spectrum x-ray imaging," *Phys. Med. Biol.* **30**, 519–529 (1985).

⁵M. Defrise, D. W. Townsend, and R. Clack, "Three-dimensional image reconstruction from complete projections," *Phys. Med. Biol.* **34**, 573–587 (1989).

⁶N. J. Pelc, "A generalized filtered backprojection algorithm for three dimensional reconstruction," Ph.D. thesis, Harvard University, 1979.